ANSTO/E707

ANSTO/E707

ANSTO

SURFACE PASSIVATION OF HIGH-PURITY GERMANIUM GAMMA-RAY DETECTOR

by

D ALEXIEV, K.S A BUTCHER,
M. EDMONDSON and E.M LAWSON

JANUARY 1993

REPORT E

ISBN 0 642-59945-9
ISSN 1030-7745

AUSTRALIAN NUCLEAR SCIENCE AND TECHNOLOGY ORGANISATION

LUCAS HEIGHTS RESEARCH LABORATORIES

SURFACE PASSIVATION OF HIGH-PURITY GERMANIUM γ-RAY DETECTOR

by

D. Alexiev, S.K. Butcher, M. Edmondson and E.M. Lawson

ABSTRACT

High purity Germanium, $/N_A - N_D/ \simeq 10^{10}$ cm^{-3}, was used for surface passivation studies. Particular experiments were made into oxidation treatment, pinch off effects and hydrogenation of dangling bonds. Passivation using hydrogenated amorphous films (a-Si:H and a-Ge:H) have been attempted. Some reduction in diode reverse current has been noted. Stability of the detector has been tested by cooling cycles to 77K with no apparent performance degradation. Moreover, the diffused contact remained intact and the detector surface did not absorb out-gassed impurities.

National Library of Australia card number and ISBN 0 642-59945-9

The following descriptors have been selected from the INIS Thesaurus to describe the subject content of this report for information retrieval purposes. For further details please refer to IAEA-INIS-12 (INIS: Manual for Indexing) and IAEA-INIS-13 (INIS: Thesaurus) published in Vienna by the International Atomic Energy Agency.

GERMANIUM, DIODE, PASSIVATION, OXIDATION, ATOMIC HYDROGENATION, PLASMA, DLTS, PINCH-OFF, SURFACE TREATMENT, RUTHERFORD BACKSCATTER, RBS, AMORPHOUS FILM

EDITORIAL NOTE

From 27 April 1987, the Australian Atomic Energy Commission (AAEC) is replaced by Australian Nuclear Science and Technology Organisation (Ansto). Serial numbers for reports with an issue date after April 1987 have the prefix ANSTO with no change of the symbol (E, M, S or C) or numbering sequence.

CONTENTS

1. INTRODUCTION

The experimental work consists of two parts. The first involves fabrication of hyper-pure germanium gamma ray detectors using standard surface treatment, chemical etchings and containment in a suitable cryostat. Then, after cooling the detectors to 77 K, γ-ray emissions from radioisotopes are resolved; resolution; depletion depth, V_R versus I_R characteristics and $/N_A - N_D/$ of the germanium are measured.

The second part of the work involves investigation of surface states in an effort to achieve long-term stability of operating characteristics. Several methods are used: plasma hydrogenation, a-Si and a-Ge, pinch-off effect and simple oxidation. All of these techniques gave some degree of passivation unique problems: a-Ge and a-Si thicknesses were measured using Rutherford backscattering techniques; surface states were measured with deep level transient spectroscopy (DLTS) and diode reverse current versus reverse voltage plots. Some scanning electron microscope measurements were used in determining major film contaminants during backscattering of a-Si and a-Ge films.

2. DETECTOR FABRICATION

A hyper-pure germanium single crystal was obtained from General Electric's Space Technology Products Division. The crystal was about 1 to 5 x 10^{10} cm^{-3} impurity concentration; it was p-type and had a <1 0 0> orientation. The crystal was cut into six sections using a wire saw with 400 mesh silicon carbide in glycerine as the abrasive slurry. The sections were then shaped and polished up to 1.2 cm diameter and up to 7 mm thickness. Damage and contamination were removed by etching the crystal for ten minutes at room temperature in a solution of 4:1=HNO_3:HF. One face of each section was then lithium diffused under vacuum by placing on a graphite plate which in turn was mounted on a heater plate inside a vacuum evaporation unit. At a pressure of 7.8 x 10^{-4} Pa (6 x 10^{-6} torr) the temperature of the plate was raised to 300°C. Lithium from a tantalum filament was evaporated on to the exposed plate and allowed to diffuse for about ten minutes. The sections were then rapidly cooled to room temperature using dry nitrogen gas. The sections were dip-etched for about 30 seconds in 4:1=HNO_3:HF to give the n^+(Li) contact.

The n^+(Li) contact was lightly lapped on glass using #600 silicon carbide and water as an abrasive. The sections were masked using Apeizon C wax and left to dry overnight. A further etch in 4:1=HNO_3:HF for about seven minutes removed any Li that might have diffused into the sides of the crystal section. The etch was quenched with methanol and the samples washed in methanol followed by drying under a dry nitrogen blower.

The p^+ contact is a layer of palladium evaporated on the opposite face from the n^+ contact and is achieved again at high vacuum in an evaporator with the n^+ contact placed onto a glass surface, thereby shielding it from the tantalum dished filament containing the Pd.

Both the n^+ and palladium contacts are masked using acid resist tape and the crystal sections are etched again in 4:1=$HNCO_3$:HF, quenched and washed in methanol, blown dry with N_2 and mounted in an Al cup, as shown in Figure 1. The diode is now contained in the Al cup which is screwed into the Cu cold finger inside the cryostat, sealed and pumped to about 2.6 x 10^{-4} Pa. After some hours of pumping, the diode is cooled to 77 K and electrical tests can be commenced.

3. METALLURGICAL EXAMINATION

One of the six sections prepared earlier from the General Electric crystal was used for dislocation studies. The crystal was grown in the <1 0 0> direction, the section was cut perpendicular to this axis, lapped with #600 lapping compound and then polished-etched in a mixture of HNO_3:HF:red fuming HNO_3=7:2:1. Dislocations were then decorated by means of a preferential etching. A mixture of $CuNO_3$ (10%):HNO_3:HF=1:1:2 was used to decorate the dislocations; this mixture has been described elsewhere[1]. A macro photograph was taken (Figure 2).

Examination of the photograph revealed etch pit density (EPD) of about 7 to 8 x 10^3 cm^{-2} and two short lineages similar to those described by Vogel[2]. The rather high EPD suggests that pronounced electrical effects could exist. Hubbard[3] found that dislocation densities of ~ 10^4 cm^{-2} give rise to two distinct bands of acceptor type levels in hyper-pure Ge. The two short lineages likewise could contribute to overall electrical deprivement of the material. Satisfactory aspects of this material are that no coring has occurred during crystal growth and there

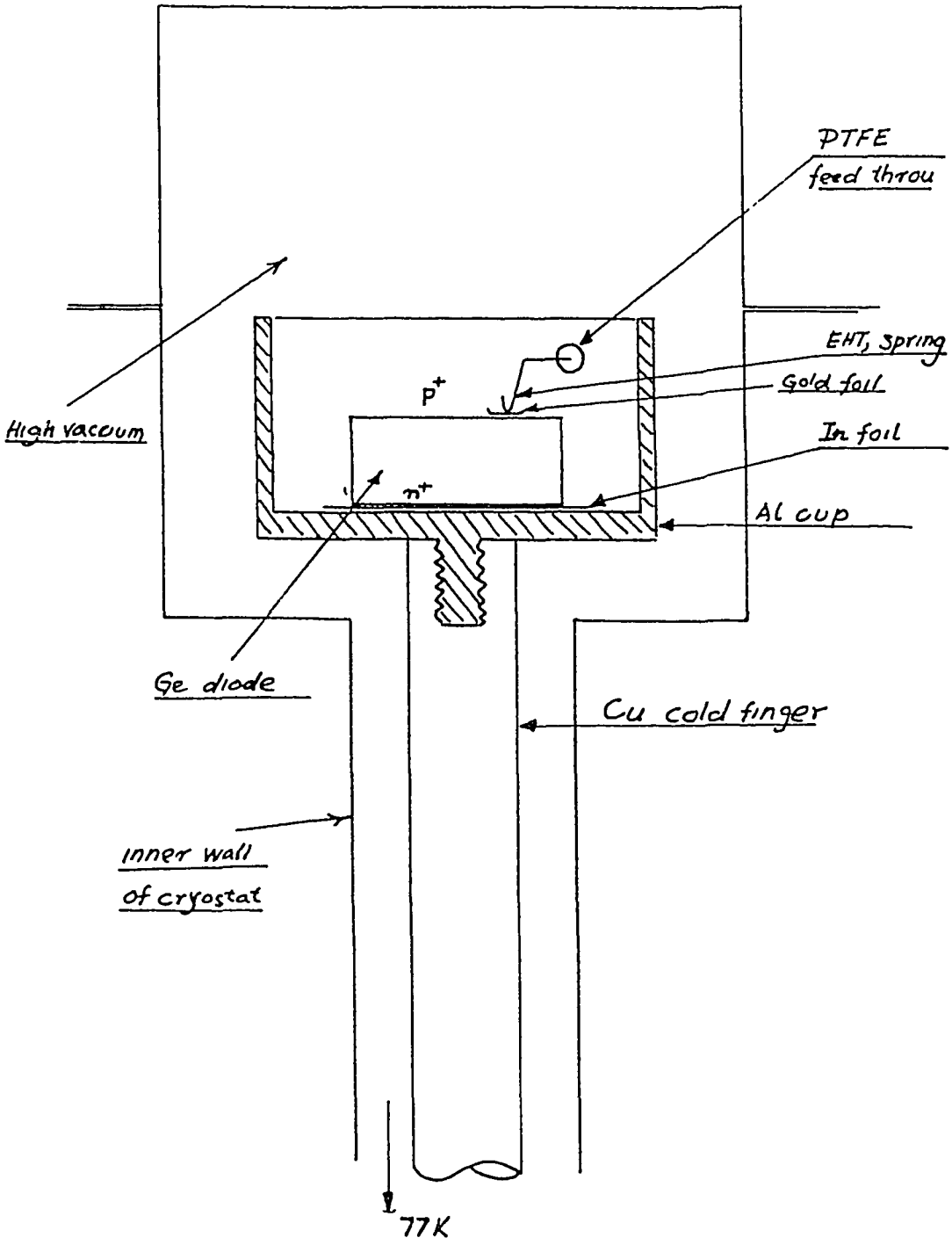

Figure 1 - Diode in Al Cup

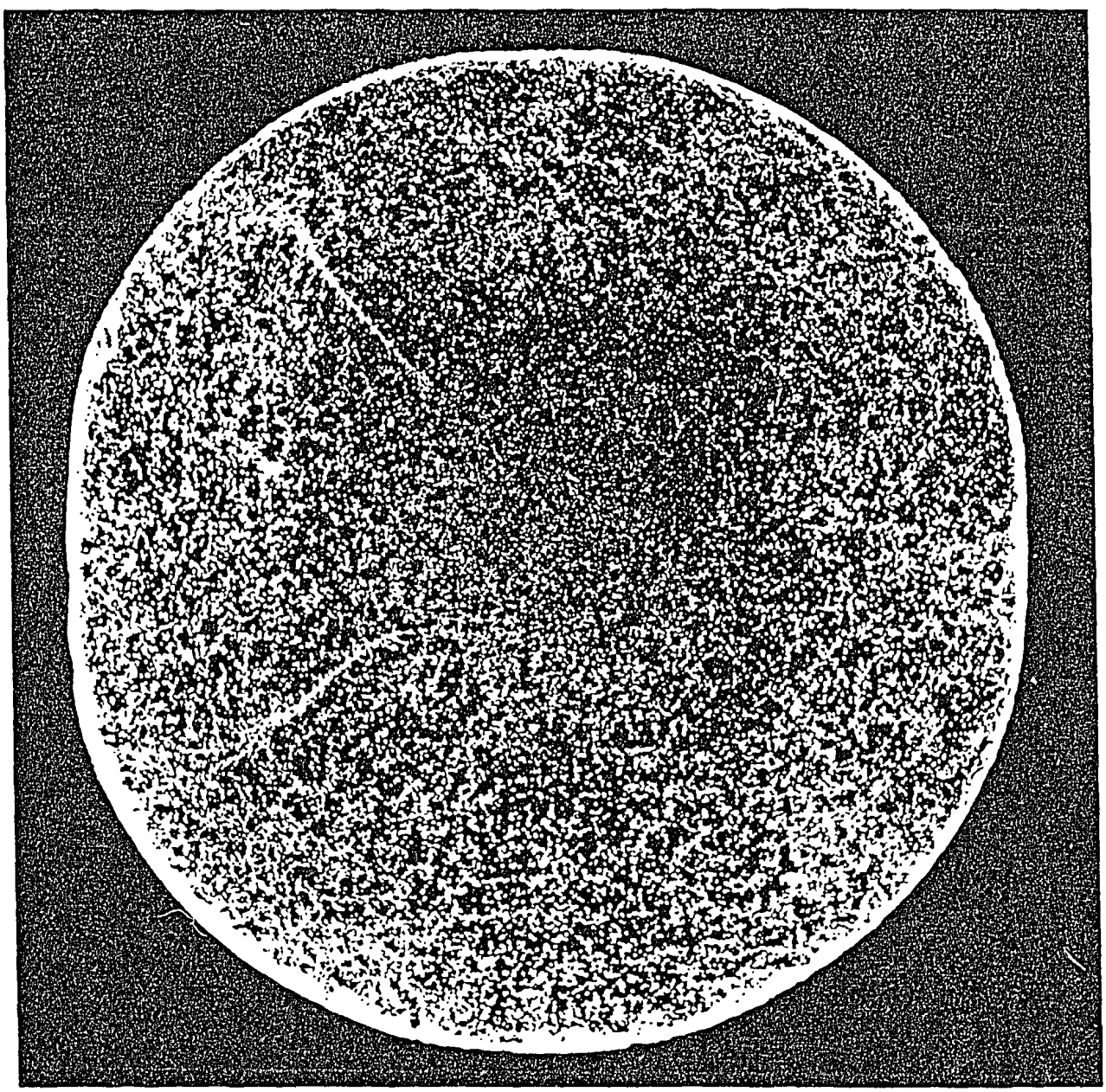

Figure 2 - Ge Dislocations, <1 0 0>, magnified x 12

is no obvious precipitation of oxides (as seen by etching) which might have been carried over from the melt.

4. THE p-n DIODE

It would be of interest to look at the transport mechanism of the p-n junction under reverse-bias before examining the experimental diodes. The leakage current I_R of a reverse-biased junction can be expressed as a sum of four current components:

$$I_R = I_d + I_{gb} + I_{gs} + I_{AV}$$

where I_d is the diffusion current, I_{gb} is the bulk generation-recombination current, I_{gs} is the surface generation-recombination current and I_{AV} is the avalanche current. The current component I_d is proportional to the minority-carrier density outside the depletion region and should remain constant for applied bias V_R greater than a few KT. Its temperature dependence should show an activation energy E_a that equals band gap E_g of c-Ge. The currents I_{gb} and I_{gs} are proportional to the respective depletion widths and, therefore, have a weak V_R dependence of $V_R^{-1/3}$ to $V_R^{-1/2}$ for a diffused junction. I_{AV} depends on the region near the junction and will depend on the level of interface state densities. I_{gs} and I_{AV} can be altered by surface passivation; ideally, the passivant must be such that it will produce flat band conditions.

The experimental diodes showed a poor V_R versus I_R characteristic, as shown in graph 1, but as often is the case, such characteristics are formed by the surface state densities (I_{gs}), by impurities such as salts left after the rinse in methanol, or by surface damage caused by earlier shaping of the crystal; not least is the surface discontinuity itself giving rise to dangling bonds. Each bond is formed by two electrons and breaking it results in two half-filled atomic states, a situation familiar from hydrogen bonding. There is an obvious chemical appeal to such a problem, in particular atomic hydrogenation of the surface. However, surface states, although arising from the breaking of specific bonds, are rather delocalised states and are spread over six to eight atomic layers, thus their charge densities cannot be associated solely with these bonds.

Repeating the etch-quench-rinse process with the n^+ and palladium contact masked with acid resist tape can eventually improve the V_R/I_R characteristic. After a number of attempts, two diodes of the initial four improved, as shown in graph 1.

Diodes number 3 and 4 produced good V_R/I_R characteristics and should fully deplete when V_R ~200 volts.

To determine the depletion voltage, a ^{137}Cs γ source was placed outside the cryostat, some 2 cm above the Al window. The intensity of the 661.6 keV line was studied as a function of applied bias to the diode. As expected, depletion efficiency increased with the increase of bias (V_R). The depletion depth of the detector (diode) is proportional to the square root of the applied bias, hence more γ-rays should be stopped per unit time as the bias is increased, until the depletion depth becomes greater than the range of the γ-ray in the germanium. At this point, saturation is reached as shown in graph 2.

From graph 2 saturation bias (V_R) was reached at 200 volts for diode number 3, but diode number 4 produced a saturation bias curve at a higher value, 600 volts.

The next parameter to be considered must be the net carrier concentration, $/N_A - N_D/$.

A plot of capacitance versus bias (V_R) was taken for both diodes, shown in graph 3.

To find the net carrier concentration for both diodes, the formula [4] $N(x) = \frac{C^3}{\rho \epsilon \epsilon_o A^2} \left(\frac{\Delta V}{\Delta C}\right)$ was used.

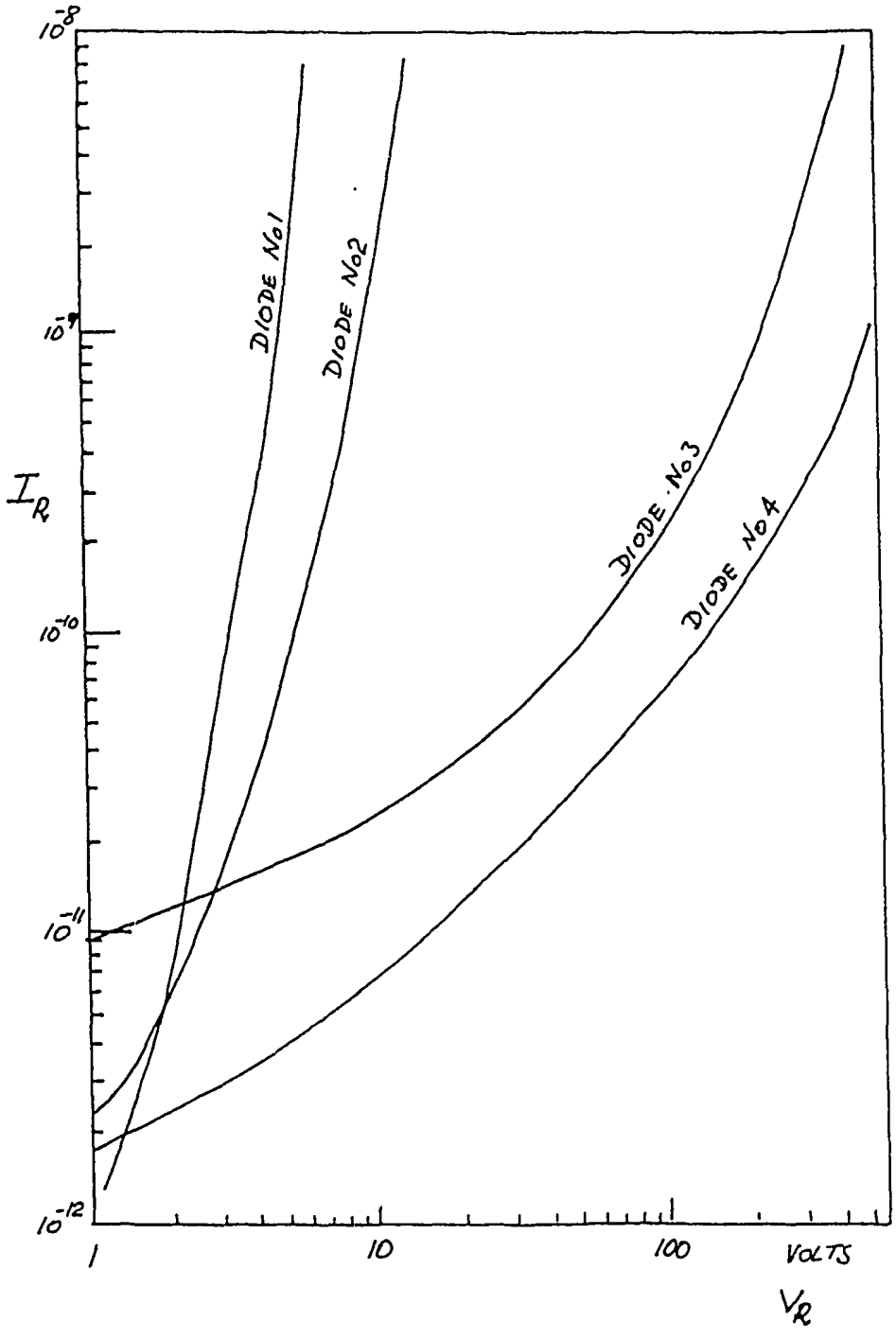

Graph 1 - $I_R(V_R)$ at 77 K

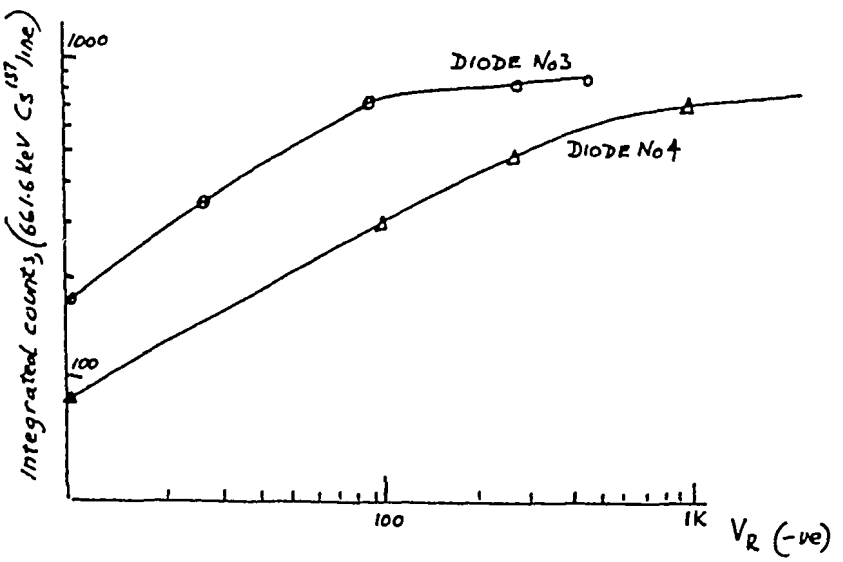

Graph 2 - Bias versus integrated ^{137}Cs γ counts

Calculations for diode number 4:

at V = 150 volts

C = 38.8 pf

ΔV = 10 volts [ΔV and ΔC values must be taken

ΔC = 7 pf at corresponding C values]

$e = 1.6 \times 10^{-19}$ C

$\epsilon = 16$

$\epsilon_o = 8.854 \times 10^{-14}$ F cm^{-1}

$A = \frac{\pi \phi^2}{4}$ where $\phi = 2$ cm

$$N(x) = \frac{34.8^3 \times 10^{-36} \times 10}{1.6 \times 10^{-19} \times 16 \times 8.854 \times 10^{-14} \times \pi \times 7 \times 10^{-12}}$$

$= 8.4 \times 10^{10}$ cm^{-3}.

A calculated value of 8.4×10^{10} cm^{-3} for $/N_A - N_D/$ was found.

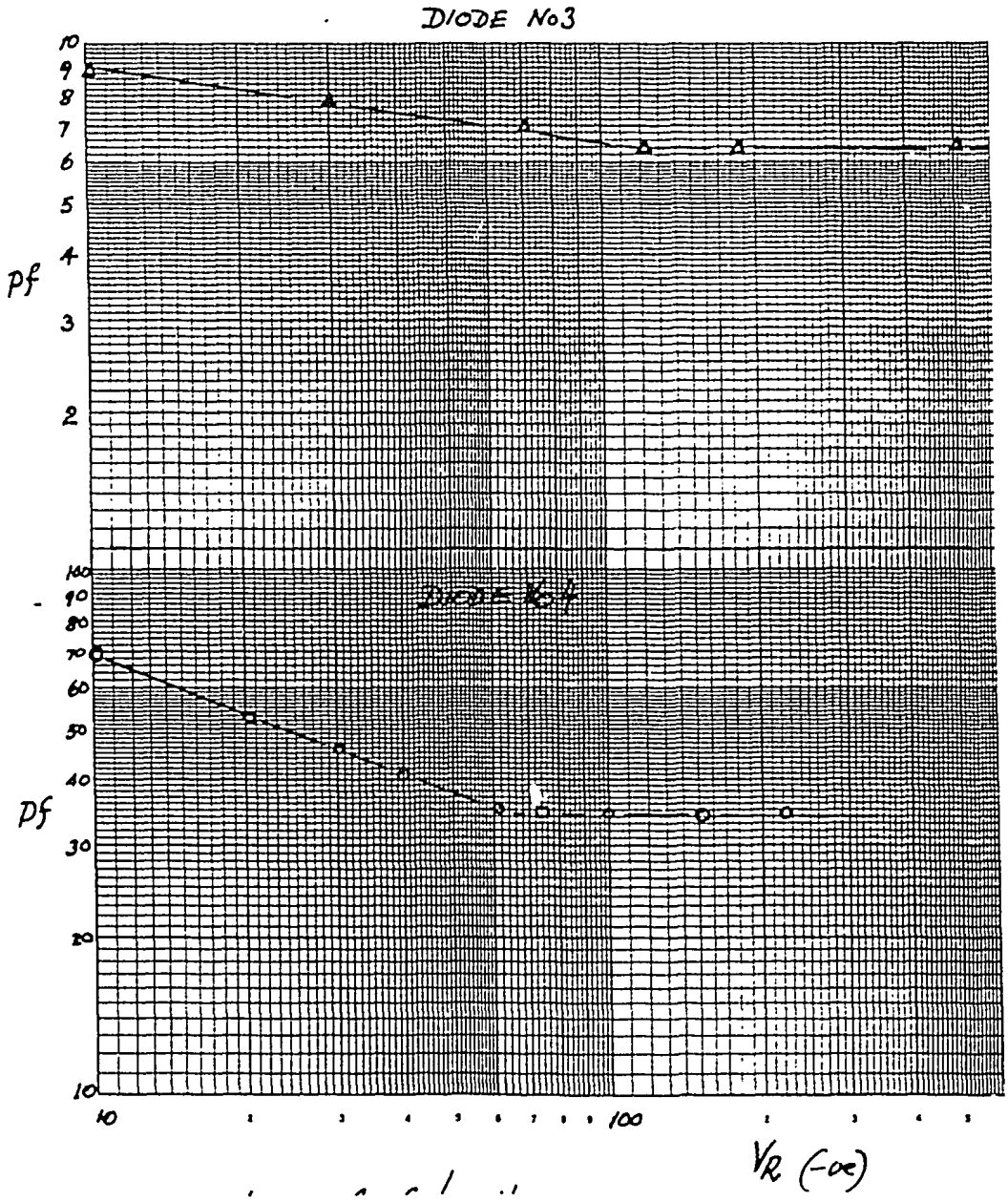

Graph 3 - Log C/Log V_R

Calculations for diode number 3:

$V = 130$ volts

$C = 6.5$ pf

$\Delta V = 16$ volts

$\Delta C = 1$ pf

$A = \frac{\pi\phi^2}{4}$ where $\phi = 1.2$ cm

$$N(x) = \frac{34.8^3 \times 10^{-36} \times 10}{1.6 \times 10^{-19} \times 16 \times 8.854 \times 10^{-14} (\pi \times 0.36)^2 \times 10^{-12}}$$

$$= 1.5 \times 10^{10} \text{ cm}^{-3}.$$

A calculated value of 1.5×10^{10} cm^{-3} for $/N_A - N_D/$ was found.

Summary	Geometry		Saturation Bias V_R	$/N_A - N_D/$
	Thickness (mm)	Diameter (mm)		
Diode No. 3	6	12	300 V	1.5×10^{10} cm^{-3}
Diode No. 4	3.2	20	650 V	8.4×10^{10} cm^{-3}

Having obtained the net carrier concentration, it is useful to relate this to the depletion depth with the aid of a standard chart for a planner diode, shown in graph 4.

5. THE p-n DIODE AS A γ-RAY SPECTROMETER

At this point of experimentation, it was decided to run the best diode as a γ-ray detector and produce spectra of some common radioisotopes. Experimental diode number 3 was used; it is fully depleted at 200 volts and has the best V_R versus I_R characteristic.

The resolution results for a number of γ emitters are tabulated in Table 1. Separate detector (due to I_R) and preamplifier (due to FET noise) can be deduced from the pulser resolution, which shows a deterioration at the high end of the spectrum, and indicates also that much of the noise width must be attributed to the preamplifier. By using selected FETs for low noise and high transconductance, the preamplifier noise width could be improved.

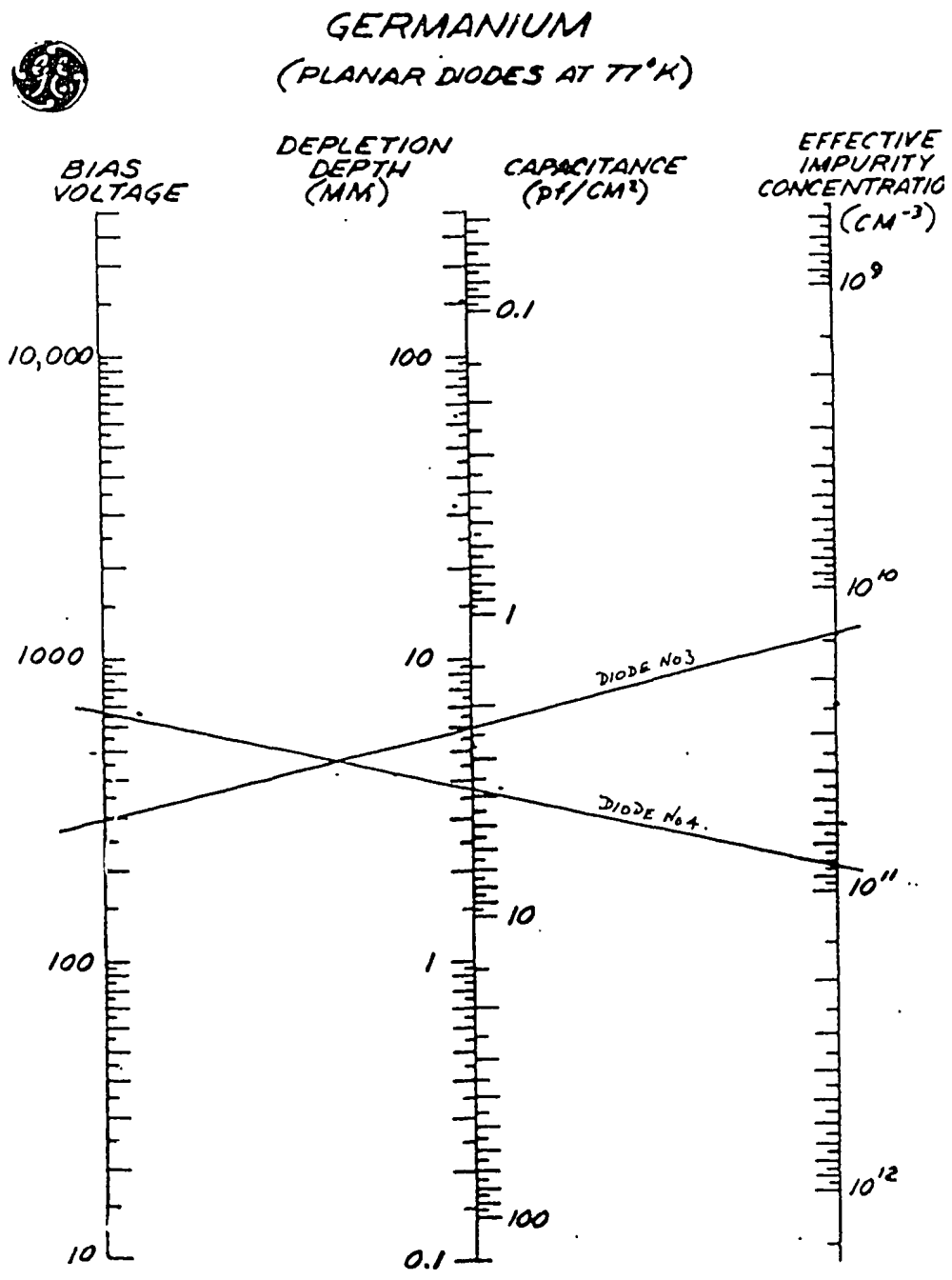

Graph 4 - Germanium (planar diodes at 77 K)

TABLE 1

Isotope	Isotope		Pulser	
	Line (keV)	Resolution (keV)	Line (keV)	Resolution (keV)
^{133}Ba	302.8	5.2	200	3.86
^{241}Am	59.5	3.15	150	3.56
^{57}Co	122	3.5	150	3.50
^{60}Co	1173	5.5	1250	5.1
^{54}Mn	834.8	4.56	740	4.21
^{88}Y	814	4.48	1000	4.41
^{22}Na	1274	4.74	1450	4.64
^{137}Cs	661.6	4.48	761.6	4.14

Further noise improvement can be achieved by remounting the input FET on a boron nitride header, attaching it on to the cold finger in the cryostat and d.c. coupling to the detector diode. Difficult it may be, but such systems have reportedly produced resolutions at 1.4 keV (FWHM) for a ^{60}Co line.

6. SURFACE PASSIVATION

6.1 Introduction

Two more current components must now be added to the earlier transport mechanism model that are affected by surface passivation and they are Ip and I(t). Ip is the current through the passivant and I(t) is the tunnel current.

Current Ip should be negligible for high resistance passivants such as a-Si or a-Ge (at 77 K) but, as was found later, these film-type passivants are only successful when evolved with atomic hydrogen. The tunnelling current I(t) must depend on V_R. Tunnelling can also occur through a combination of thermal excitations and field emissions through gap states. The activation energy will then depend on the energy distribution of the gap state; it will be higher for transitions mostly through deep states than those mostly through shallow states.

Figure 3 shows the band structure of c-Ge with a superimposed a-Si:H or a-Ge:H film with V_R applied.

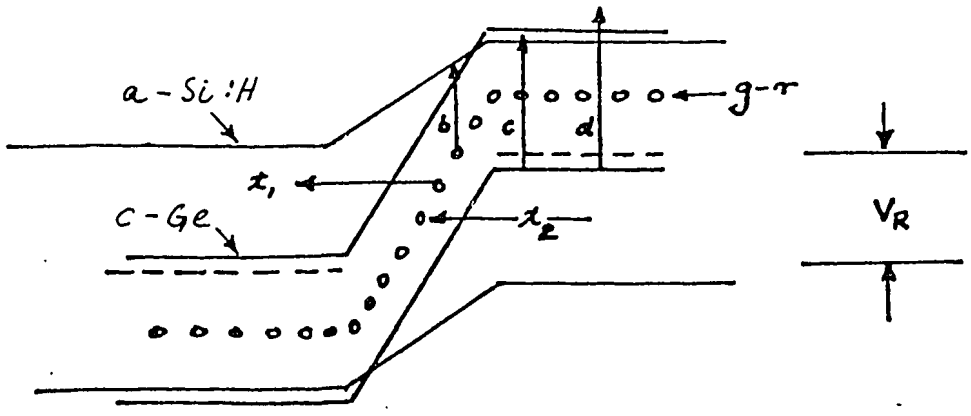

Figure 3 - Band structure of c-Ge with a superimposed a-Si:H or a-Ge:H film with V_R applied

Under reverse bias, electrons from the g-r centres can tunnel out to the conduction band of c-Ge(t_1), but cannot go to the conduction band of a-Si:H or a-Ge:H because of the higher energy required. Similarly, only electrons from the valence band of c-Ge can tunnel to the g-r centres. Thermal activation (processes a and b) can populate the conduction band of c-Ge and the conduction band of a-Si:H or a-Ge:H and would constitute a leakage of interfacial electrons.

In this section bias stress on I_R will be examined as different passivants are tried. Bulk currents such as I_d and I_{gb} can be assumed not to be affected by the use of different passivants, therefore I_R will be sensitive to I_{gs} (surface generation-recombination current), Ip (current through passivant) and I(t) (tunnel current).

Several different passivation techniques are used; the first, the simplest, is buffer ring protection and oxidation. This is followed by hydrogenation of the surface, sputtering and deposition of a-Si:H and a-Ge:H.

6.2 Buffer Ring Protection and Oxidation of the Diode Surface

Experimental diode number 3 was used for this experiment. It was observed that, after repeated etches, small fragile knife edges were formed on the boundaries between the protected ohmic and n^+ layers and the side walls. These knife edges can easily be broken off or simply damaged during fabrication. A buffer ring can act as an electric singularity zone where the electric field lines concentrate. This concentration, in turn, relaxes the field gradient at the edge of the n^+ contact (recalling that the diode is p-type material V_R will therefore deplete from the n^+ contact). For the buffer ring to be efficient it must be cut as close as possible to the n^+ edge.

The buffer ring was fabricated first using 4:1 HNO_3:HF etch. The crystal was totally covered with etch resist tape, except for a 1 mm strip around the periphery. The etch process was for some ten minutes, but proved unsuccessful, due to minute bubbles forming inside the strip causing uneven and abrupt etch patterns. This method was repeated several times, including placing the etch and masked crystal into an ultrasonic bath so that the bubbles could be rapidly dispersed, but no major improvement was noted in the appearance of the etched groove. The buffer ring was finally and successfully formed using a 0.5 mm thick diamond saw and a rotating platform to which the crystal was centrally attached. A groove 1 mm deep was cut, as shown in Figure 4.

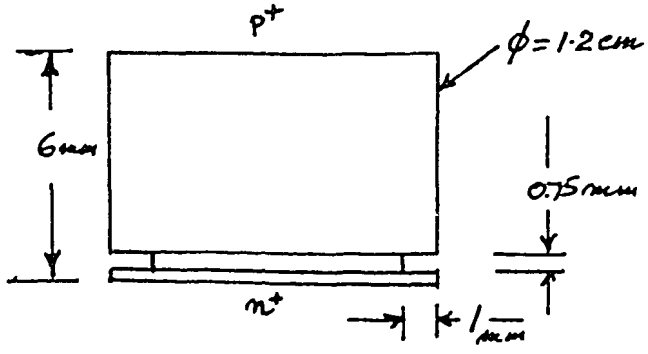

Figure 4 - Buffer ring cut on a diode surface

The p^+ and n^+ contacts were masked and the diode etched in 4:1 = HNO_3:HF, quenched and rinsed in methanol.

After mounting the diode in the cryostat, pumping and cooling it to 77 K, a V_R versus I_R plot was made, as shown in graph 5. It showed a poor V_R/I_R characteristic, which prompted the oxidation of the surface as well [5]. The oxidation etch proceeds in three stages. Firstly, the device (palladium and n^+ contact masked) is placed into a solution of 1:1 HF:H_2O_2 at 30°C. A slight colour change is noted in its metallic lustre. After one minute, HF is added so that the mixture becomes 2:1 HF:H_2O_2. The surface now shows faint interference colours. Again, one minute later, HF is added so the solution is 4:1 HF:H_2O_2. At this point, the surface changes colour to a yellow film, under which is the oxide layer being translucent grey in appearance. After the diode is quenched and rinsed in methanol, the yellow film is removed either with a cotton swab or by ultrasonic agitation.

The diode is again placed into the cryostat, pumped and cooled to 77 K. A V_R/I_R plot is taken and the result is shown on graph 5. A marked improvement is noted.

During the cooling period of the diode, ambient water vapour inside the cryostat could condense on the diode surface. For this reason, it was decided to go through a number of heat-pump-cool cycles.

The cryostat was raised to 373 K and pumped at that temperature for four hours, after which it was cooled to 77 K. The diode was cycled twice in this fashion. V_R/I_R plots made produced excellent characteristics (graph 5).

It is now of interest to test the resilience of the oxide layer. This is accomplished by placing a 2 cc beaker with H_2O inside the cryostat. After the cryostat was evacuated, a partial vapour of H_2O was produced. Four days later, the diode was re-examined and showed a marked deterioration in its V_R/I_R characteristic. The diode was subjected again to the heat-pump-cool cycle and a further plot of V_R/I_R showed that the diode returned to its previous state.

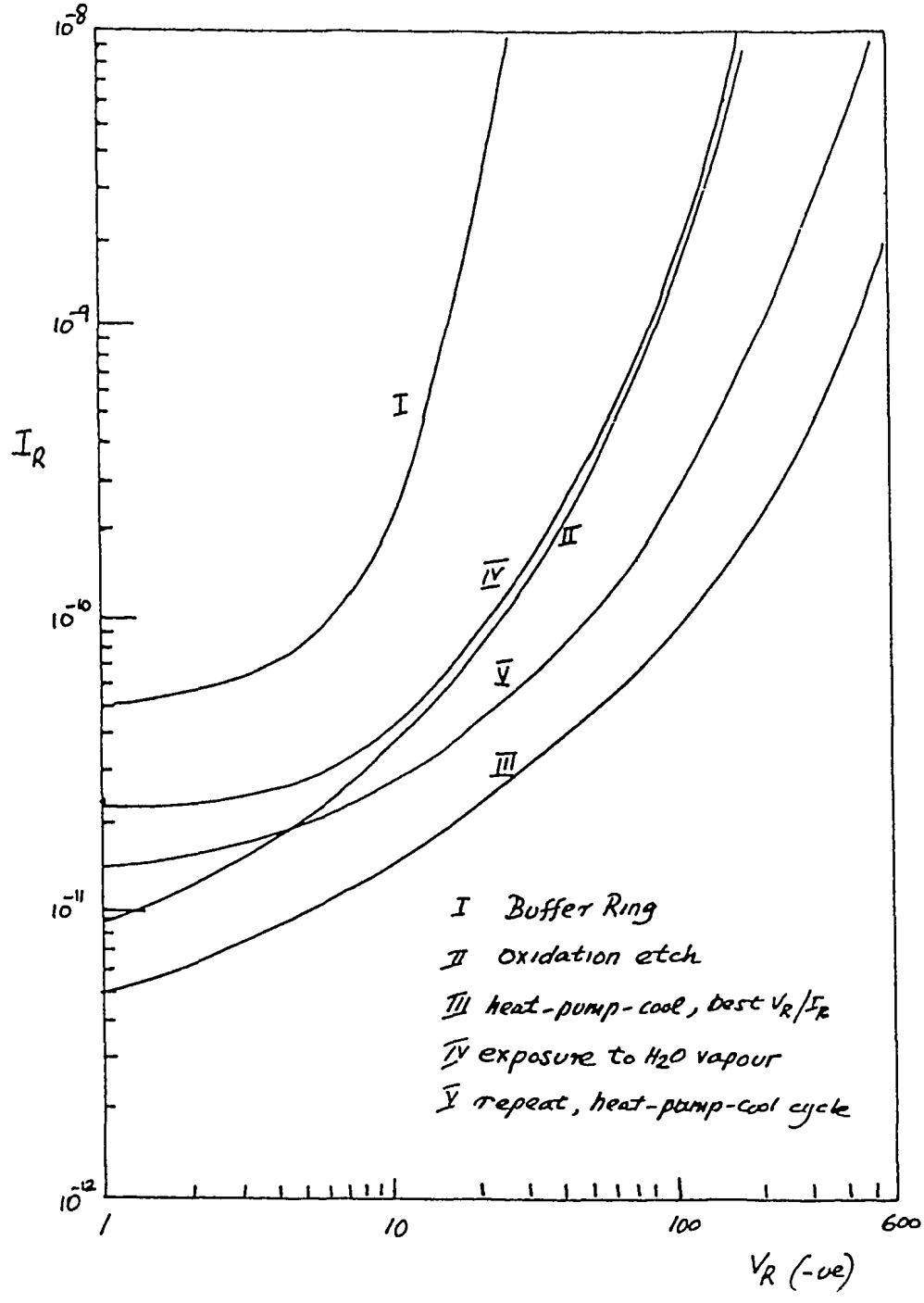

Graph 5 - V_R versus I_R for buffer ring, oxide etch and heat-pump-cool cycle

Several thoughts came to mind after this experimentation; firstly, the buffer ring should have had some influence on improving characteristics, but none were seen (three more diodes fabricated with the buffer ring showed little improvement). The oxide layer treatment produced excellent results, but proved to be not impervious to water vapour which would be the major contaminant when the diode is stored at ambient temperature and pressure.

6.3 Hydrogenation of the p-n Surface

The ability to hydrogenate (atomic hydrogen) dangling bonds has been extended to c-Si and c-Ge[6]. They have shown that after a surface is exposed to atomic hydrogen a dramatic drop in leakage current (I_R) can be observed. With this in mind, a hydrogenation experiment was designed.

The sorbate-sorbent interactions between two molecular species normally have heats of absorption much higher than that associated with van der Waals bonding. Energies of such interactions can be equated to a chemical reaction between the adsorbate gas and the absorbent (crystal surface). It follows that when such strong interactions occur, the adsorbing molecule must change its structure. Molecular H_2 cannot be expected to be strongly adsorbed unless it is dissociated into its two H atoms. Energy has to be fed into the H_2 gas for dissociation to occur; this can normally be achieved by high temperatures, high d.c. voltage, or more simply, by using an RF field. In this experiment 27.5 MHz was used. Such a system was developed by the authors for this experiment, and is shown schematically in Figure 5.

An 800 watt 27.5 MHz RF generator couples energy into a quartz column containing a partial pressure 93 to 106 Pa of H_2. The molecular hydrogen is supplied via a palladium diffuser, since ordinary tank hydrogen can contain unacceptable impurities such as H_2S which would constitute a dopant. Inside the quartz column is a heater pedestal with an intrinsic Ge section used to hold and heat the Ge diodes. The instrinsic Ge base and heater pedestal is shrouded with a quartz tube. The vacuum system consists of a rotary pump, a 1201 s^{-1} turbo molecular pump, a throttle valve and an ℓN_2 trap just below the heater pedestal. The heater can be controlled from ambient to 400°C at a resolution of ½°C using an Ether minicontroller, series 1990.

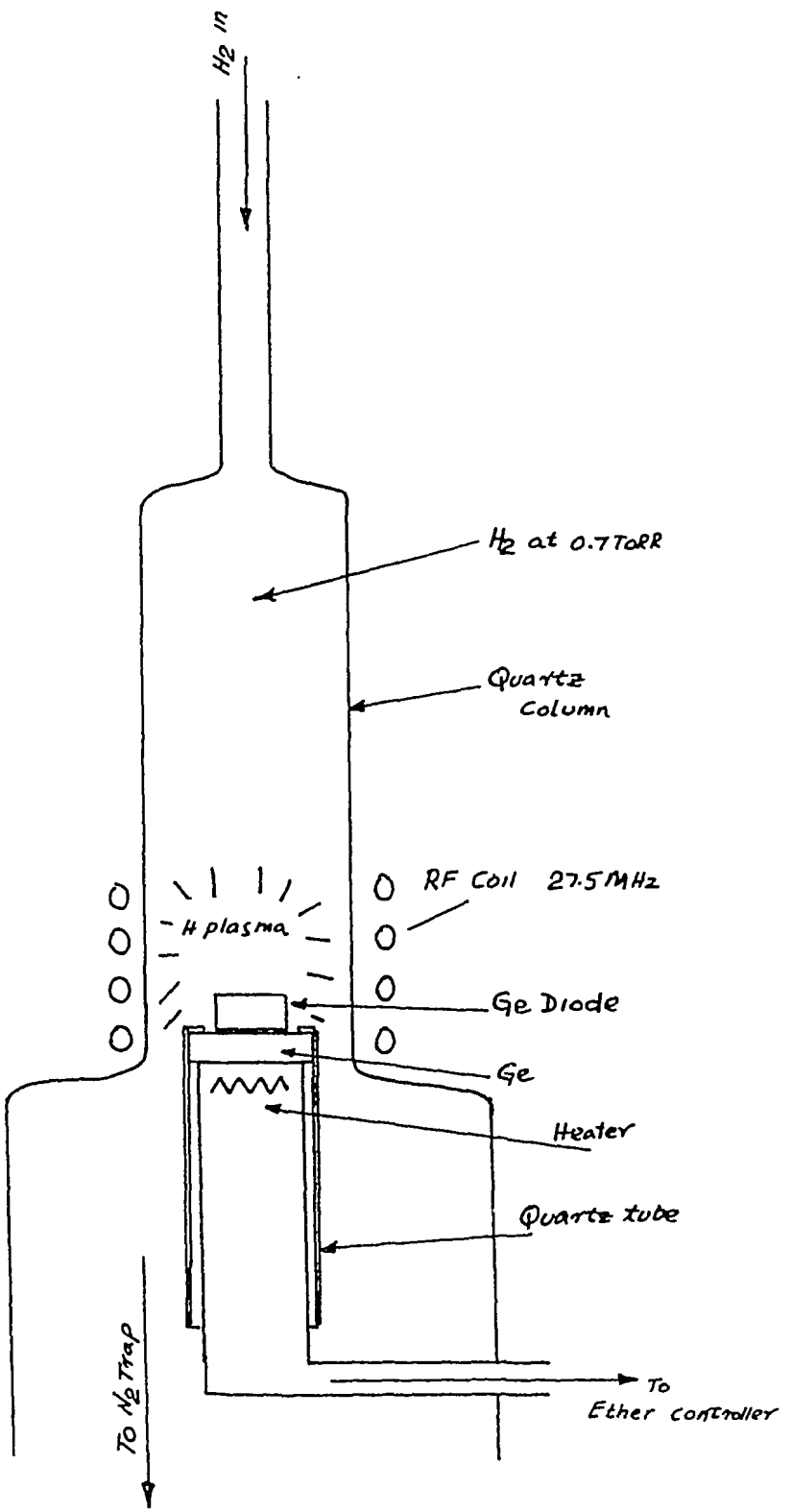

Figure 5 - Hydrogenation of a p-n surface

Two more hyper-pure Ge diodes were constructed for this experiment. The ohmic and n^+ contact was formed as described previously. The diodes were cooled to 77 K and a V_R/I_R plot was obtained. Afterwards, the diodes were placed in turn into the hydrogenation column with the ohmic contact facing down onto the Ge topped heater pedestal. After a partial pressure of molecular hydrogen was established (93 to 106 Pa), the RF generator was switched on and adjusted to a power output of 4 watts, an intense plasma of atomic hydrogen was obtained forming a column of approximately 50 cc. The heater was switched on and held at a temperature of 600 K for 15 minutes and then switched off. Once back at ambient, the RF generator was switched off. The diode was again checked for its V_R/I_R characteristic which can be seen in graph 6. It can be seen from the graph that the diodes were originally quite leaky, possibly indicating the presence of a large number of dangling bonds, and were particularly suitable for this study. Again, from the graph, it can be noted that after hydrogenation the reverse bias characteristic showed a dramatic drop in I_R.

It is now of interest to revert the diode to its initial state (poorer I_R) by dehydrogenation. This was done by simply heating the diode at 600 K in vacuum (1.3×10^{-4} Pa) for about one hour rather than the 15 minutes taken earlier for hydrogenation, since it is possible that a longer time is needed to dissociate a complex molecular species than to form it. Again, the reverse bias characteristic at 77 K showed an incomplete reversal to the initial state, as shown in graph 6. It can be concluded that a detailed study has to be made into temperature versus time of hydrogenation and dehydrogenation to optimise this process.

6.4 a-Ge:H and a-Si:H Film Deposition on Quartz

Sputtering is one of the more popular processes for deposition of thin films; in particular, such techniques are used in thin film solar cell construction[7] and passivation of coaxial germanium detector surfaces[8].

A large diameter quartz column assembly was designed for this experiment, as shown in Figure 6. Large areas of Ge and Si targets can be used. In this experiment, a 5 cm diameter Ge and a 4 cm diameter Si poly-crystalline section was used. The ionising voltage is applied by a 20 mA, 10 kV EHT unit. The film substrates are 1 x 2 cm by 1 mm thick quartz sections. The sputtering gas in argon mixed with 10% hydrogen at a partial pressure of 1.3 Pa.

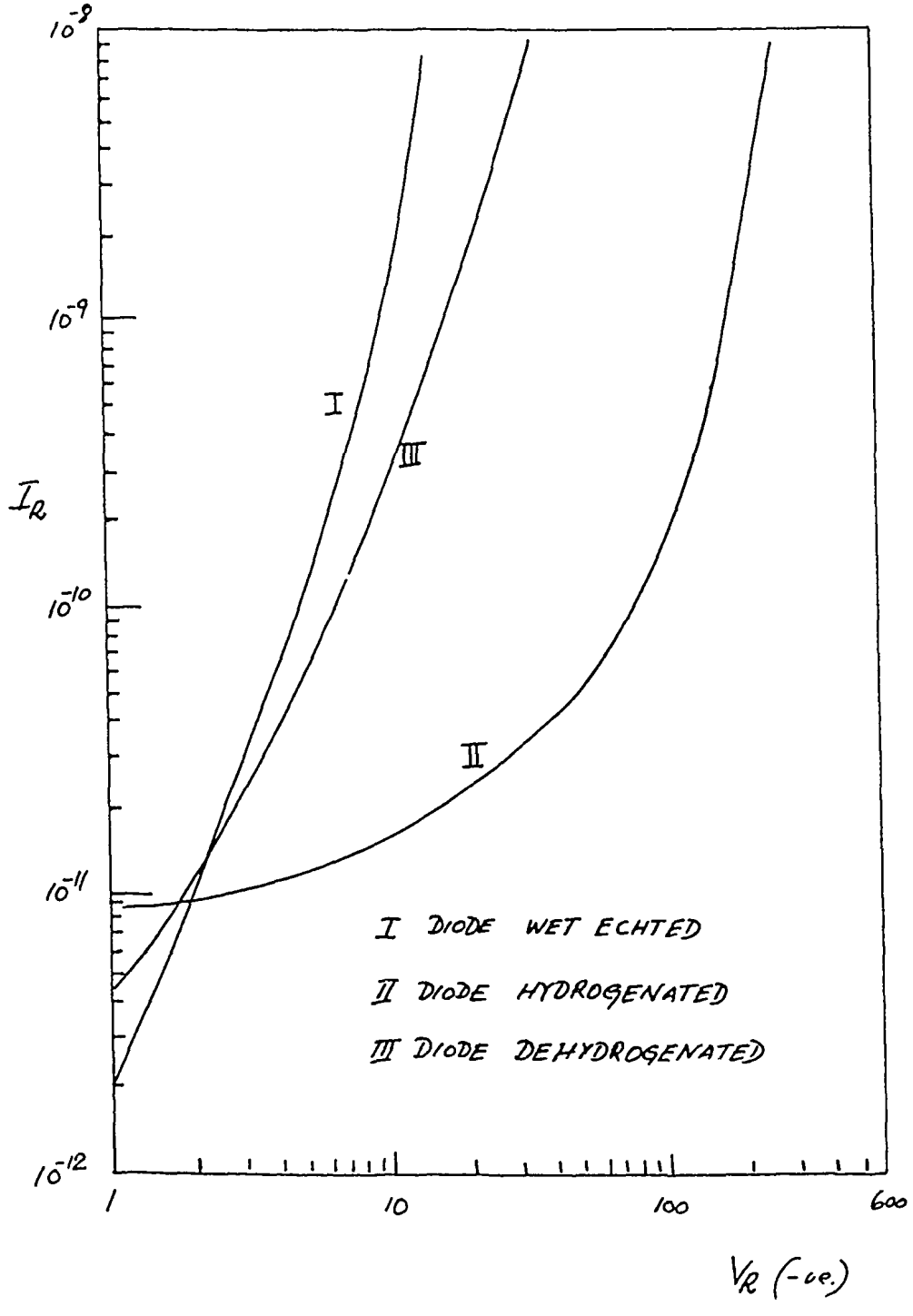

Graph 6 - V_R versus I_R for a 'wet' etched, hydrogenated and dehydrogenated diode surface

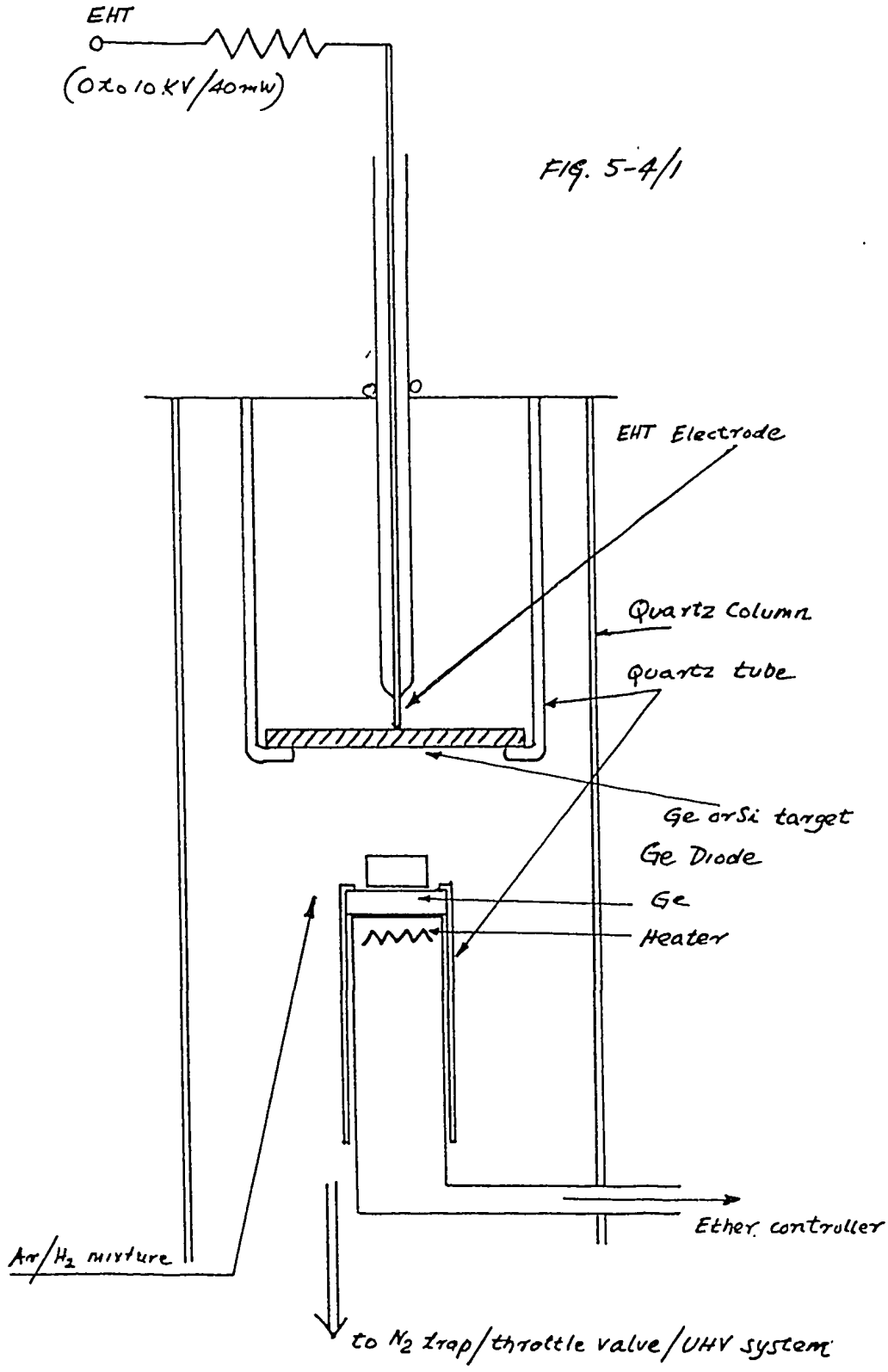

Figure 6 - Schematic of the sputtering column

The procedure is firstly to wet etch the quartz sections. After quenching and rinsing in methanol, they are placed on the heater pedestal. The sputtering chamber is then pumped for about one hour at a vacuum of 1.3×10^{-4} Pa. Argon is mixed with 10% of pure hydrogen, then admitted and left to stabilise at approximately 1.33 Pa. EHT is applied (-ve on target), normally at 6 kV/4 mA for times ranging from half an hour to two hours.

Film thicknesses and therefore deposition rates are measured using Rutherford backscattering (RBS) techniques. All the RBS measurements were done on the 3 MeV accelerator at Lucas Heights.

It is worth noting that RBS experimental arrangements are straightforward, simply involving collecting and analysing high energy particles rebounding from the target specimen. Energies above 2 MeV are normally used to penetrate films such as the amorphous layers of Ge and Si. Two parameters can easily be obtained from the RBS spectrum: firstly, the concentration of impurity elements, particularly high mass elements, and secondly, target thicknesses. Graph 7 is an energy spectrum of RBS and graph 8 is the same spectrum, but at a higher gain setting. The graphs show analyses of an a-Ge:H film on quartz.

RUTHERFORD BACKSCATTERING OF a-Ge:H FILM ON QUARTZ

	Peak	Channel No.	Source
Major	Si	266	quartz
	O	167	quartz
	Ge	393	a-Ge film
Minor	Ar*	330	pmm level of impurity
	In(?)+	420	pmm level of impurity

* The argon impurity can be explained as a gaseous inclusion during deposition of the film.

\+ The In(?) contamination possibly from an earlier run where In was used.

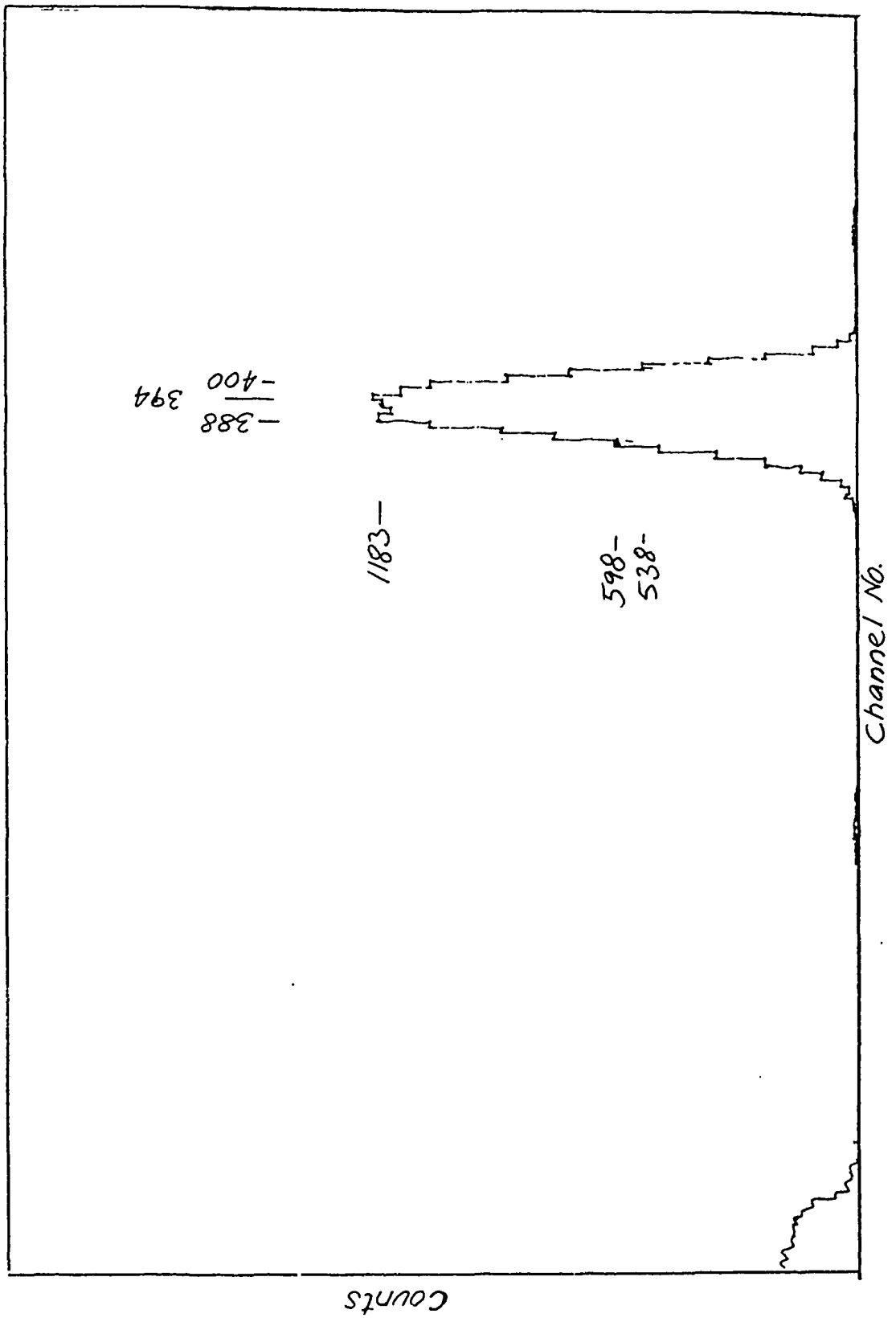

Graph 7 - Rutherford backscattering spectra of sputtered a-Ge on quartz.

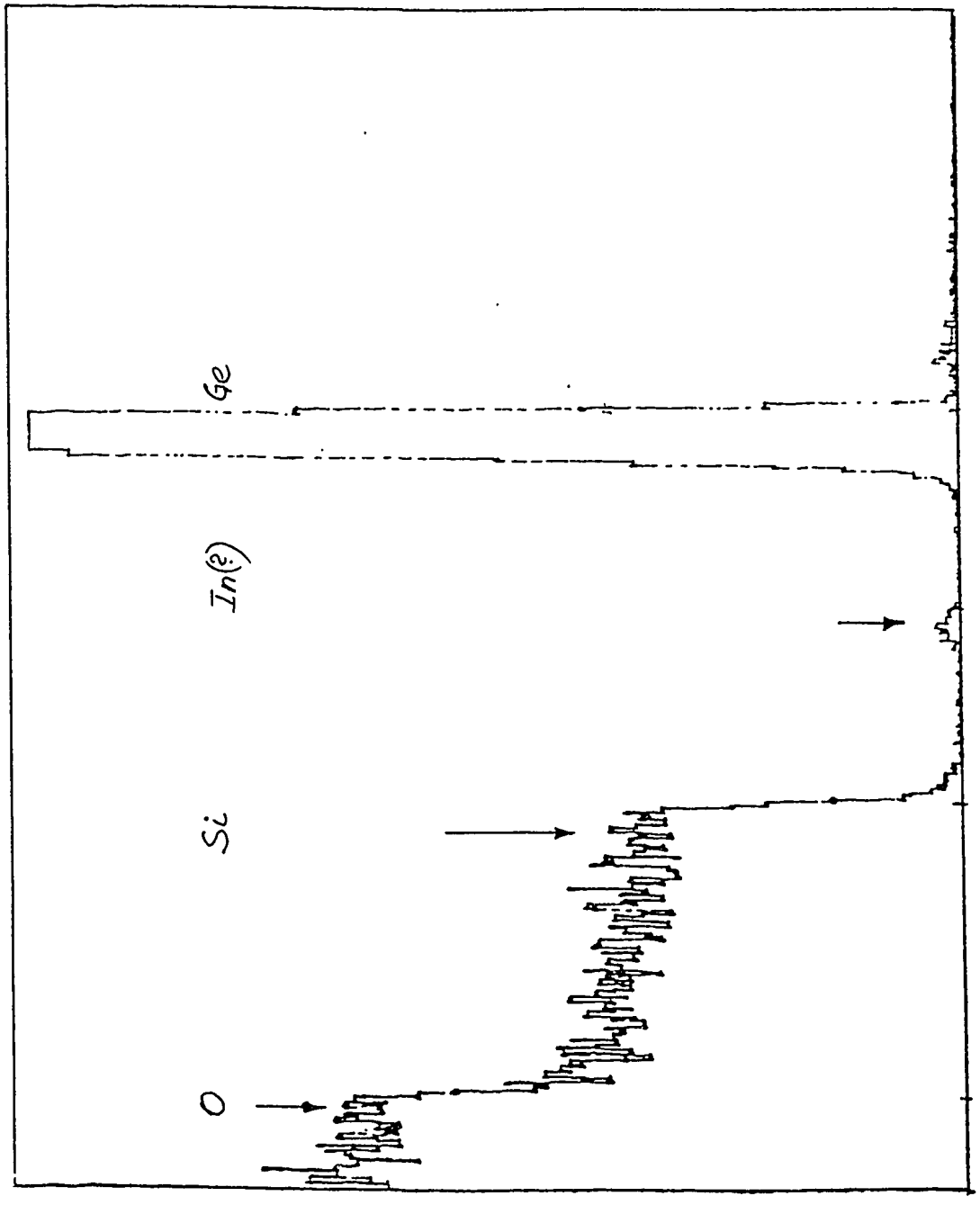

Graph 8 - Amplified version of Graph 7, showing O, Si and Ge with possible In inclusion

Thickness calculation of the a-Ge:H film

FWHM	≈	12 channels
Allowing for detector resolution $(12^2-3.5^2)^{\frac{1}{2}}$	=	11.5 channels
Therefore width of Ge peak	=	3.95 keV/channel
Conversion to thickness		60.5 eV/Å from Table IX, ref (9).
Therefore thickness is $\frac{11.5 \times 3.95 \times 10}{60.5}$	=	750 Å

Sputtering data for a-Ge:H on quartz

Time = 1½ hours

EHT = 6000 V

Ag:H = 9:1

Which makes the deposition rate at 8.3 Å per minute; a similar deposition rate was obtained for a-Si:H.

Both films were subject to bias stress at ambient temperature and also at 77 K. A plot was made of I(V) shown in graph 9. From the graph it can be concluded that the amorphous film when deposited on the p-n surface (at 77 K) should have negligible current contribution to sheet resistivity (I_R).

When tested for mechanical durability the films showed remarkable resistance to abrasion and scratching with a sharp point. a-Ge:H film has a light cobalt blue appearance; a-Si:H has a green-yellowish appearance.

6.5 Passivation of the p-n Surface with a-Si:H and a-Ge:H

Surface states altered with amorphous films are analysed using a relatively new and powerful technique: deep level transient spectroscopy (DLTS). Such a spectrometer was built by the one of us and colleagues[10,11]; the system sensitivity has been measured to better than 6×10^{-5} of the background doping density of the devices.

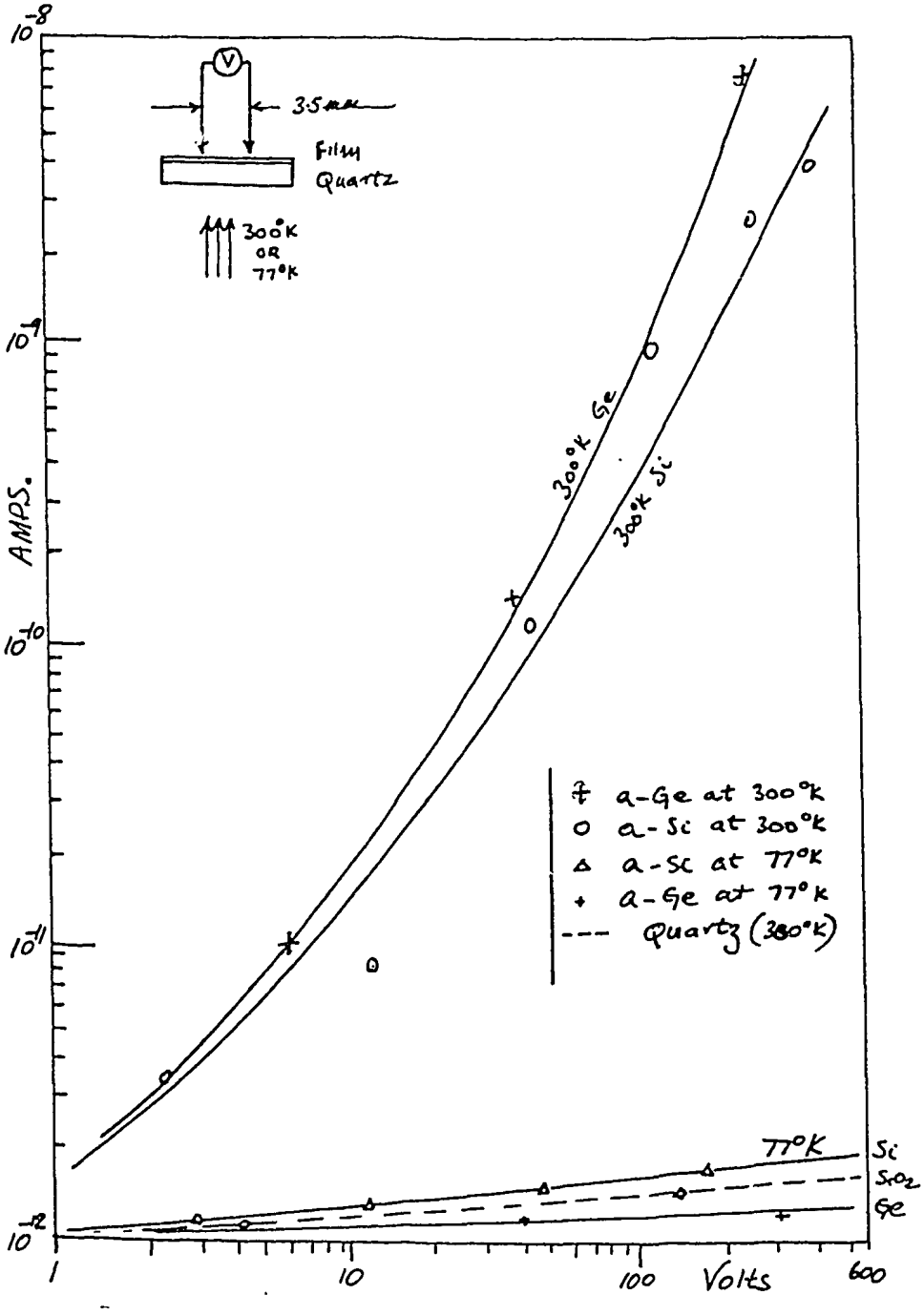

Graph 9 - Bias stress I(V) of sputtered films

It would be in order to review briefly the DLTS. Significant advances were made by Lang (1974)[12] in detecting and characterising deep level trapping centres in semiconductors. DLTS uses the repetitive pulsing of bias on a p-n junction or Schottky barrier structure to change the space-charge (depletion) depth. Defect states are filled during the pulses and may empty between the pulses if the temperature is high enough to provide sufficient thermal energy for detrapping. The resulting capacitance transients are processed by a correlator[13] set to a specific exponential time constant. As the sample temperature is scanned, a peak in the correlator output is obtained when the time constant of the capacitance transient is coincident with the internally generated exponential weighting function of the correlator.

By measuring (a) the change in temperature at which a peak is observed with a corresponding change in weighting time constant, the activation energy for carrier emission from the defect state may be obtained; (b) the decrease in correlator output as the bias pulse width (the trap filling time) is reduced, the capture cross section may be measured; and (c) the change in the magnitude of the capacitance transient with a change in the bias pulse amplitude, i.e. the distance over which traps in the lightly doped side of the junction are filled, the concentration profile of the defect is obtained.

A full review of the theory is given in the references[14].

A fundamental limitation occurs when the capacitance of the test sample does not change significantly with V_R. This has been overcome[10] monitoring the transient conductance when detrapping from a defect centre occurs. This is achieved by adding a calibrated delay to the phase sensitive detector in the capacitance bridge so that the bridge is detecting conductance changes.

The experimental procedures for depositing the amorphous film onto the diode surface are similar to the method described earlier. Since the palladium contact is fragile, it is shielded from the sputtering gas action by inverting and placing it onto the Ge substrate located on the heater pedestal. A description of the method follows:

1. Firstly, the system is evacuated to 1.3×10^{-4} Pa;
2. A mixture of Ar and H_2 is admitted in a ration of 9:1; it is throttled and left to stabilise at 1.33 Pa;
3. The heater is switched on and set to control at 200°C;
4. EHT is applied to the target; normally 6 kV is used; and
5. Time for deposition is about one hour, thereby yielding a surface film of 500 Å thick.

Figure 7 shows a schematic of (a) deposition of amorphous hydrogenated films of Ge or Si and (b) sputter cleaning diode surface. Amorphous Ge:H and a-Si:H has been applied in such a manner to five diodes with repeated alteration to initial surface conditions.

Typical results for a-Ge deposition

Initial surface preparation

Wet etch 4:1=HNO_3:HF, methanol quenched and rinsed.

Wet etch and sputter cleaned for ten minutes.

Sputter cleaned only on aged wet etched surface.

Film deposited

500 Å thickness using

- Ag + 10% H_2
- Ag + 30% H_2
- Ag + 40% H_2

$I_R(V_R)$ at 77 K

All cases resulted in poor characteristics quite unsuitable as a detector.

DLTS spectrum

Two series of DLTS spectra are taken.

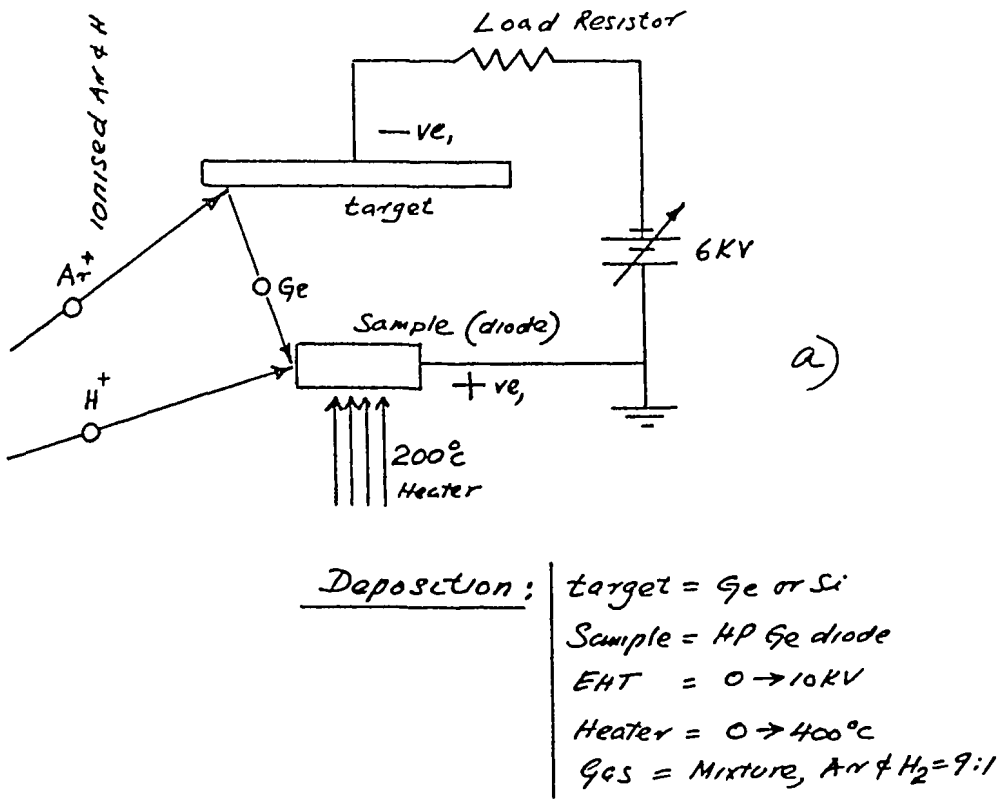

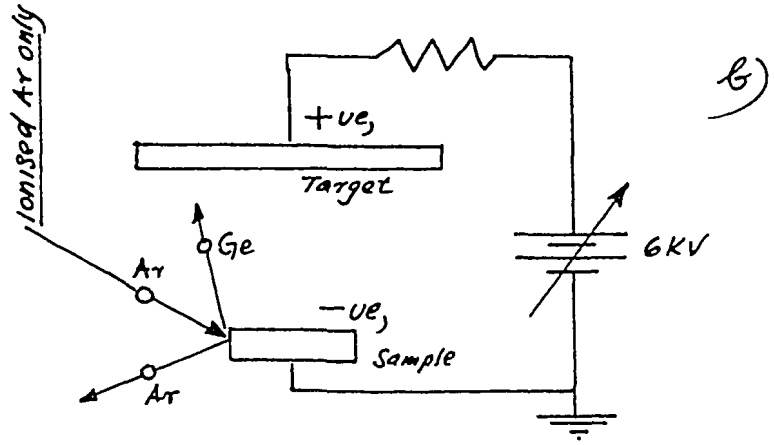

Figure 7 - (a) Deposition; (b) Sputter cleaning diode surface

DLTS before a-Ge:H film deposition - shown on graphs 10 and 11. Graph 10 shows a scan, 2.5 mm deep into the bulk of the diode. It shows (a) hole (acceptor) trap at density N_T = (2 x 10^8 cm^{-3}) at a level of Ev + 0.14 eV, possibly Ni impurity, (b) electron trap at density N_T = 2 x 10^8 cm^{-3} at a level Ec - 0.13 eV which can be explained as a process induced donor since it is situated near the Li diffused contact, possibly Ni-Li complex because of similar concentration level. Graph 11 shows a scan of full depletion depth of the diode. It shows a hole trap density N_T at about 3 x 10^8 cm^{-3}, consisting of possibly one Ni impurity and two Ni-Li complex peaks. Again, its level is Ev + 0.14 eV.

DLTS after a=Ge:H deposition - shown on graph 12(a). This graph shows a scan of surface defects; it will be recalled that for surface DLTS scans an infrared LED is used to inject pulsed minority carriers. The scan shows a hole trap density (N_T) at 1.6 x 10^9 cm^{-3}. This constitutes a background doping density of $\simeq$ 10% of the bulk density where $/N_A - N_D/$ = 1.4 x 10^{10} cm^{-3}. Thus the poor ($I_R(V_R)$ characteristic can be understood.

An attempt was made to neutralise these defects.

1. The diode was heated at 150°C in 2.6 Pa of H_2 for half an hour. This resulted in no change in the DLTS spectrum (shown on graph 12(b)).
2. The diode was again heated at 150°C for 1.5 hr, but this time in atomic hydrogen (93 Pa, 40 watts, 27 MHz RF), power density at about 1 watt per cm^3.

The DLTS spectra showed all hole defects had been removed, as shown on graph 12(c).

A further bias stress plot, $I_R(V_R)$ at 77 K showed that the diode had improved, but not to an acceptable level to be used as a detector.

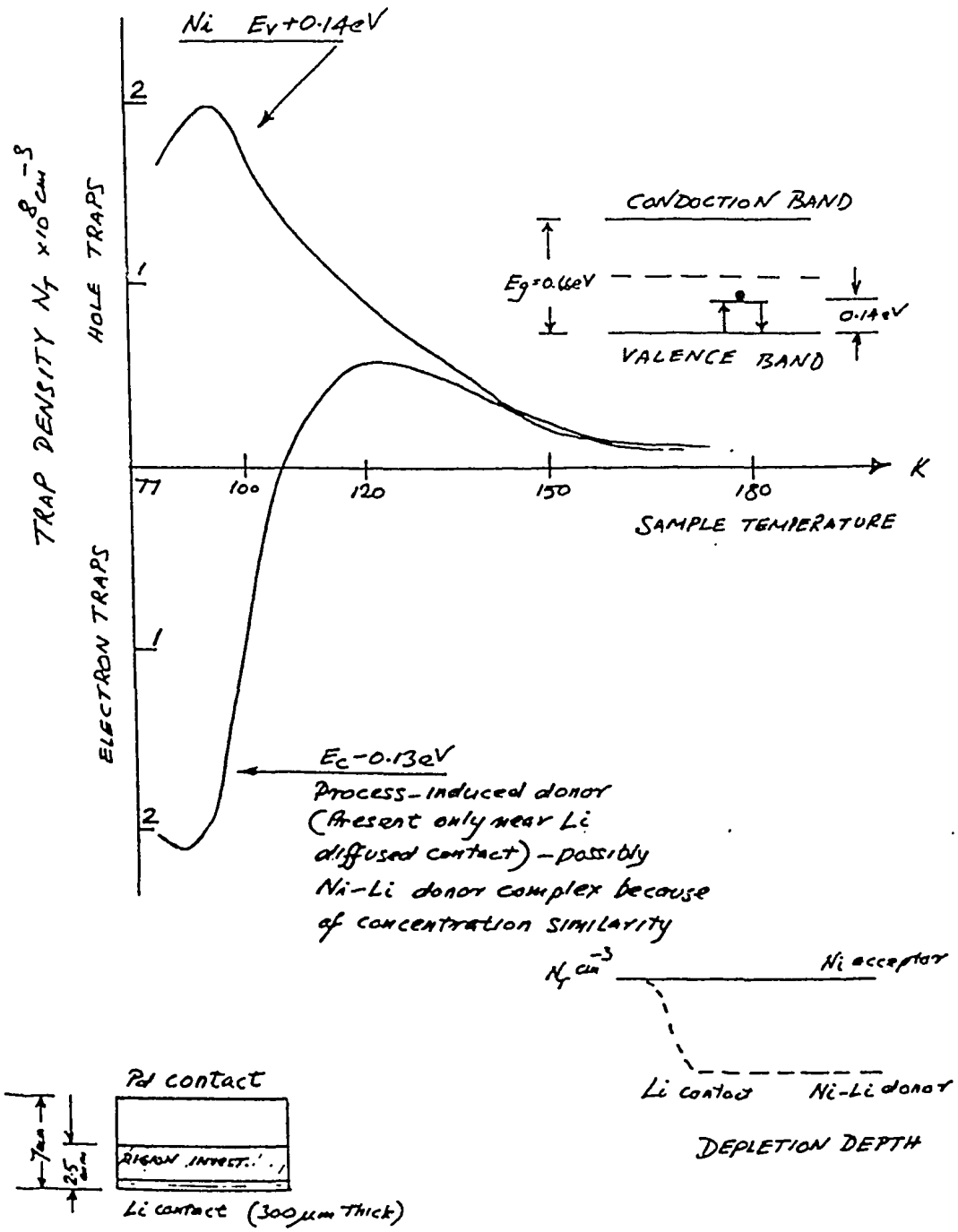

Graph 10 - DLTS scan of HP p-Ge detector diode (2.5 mm into bulk)

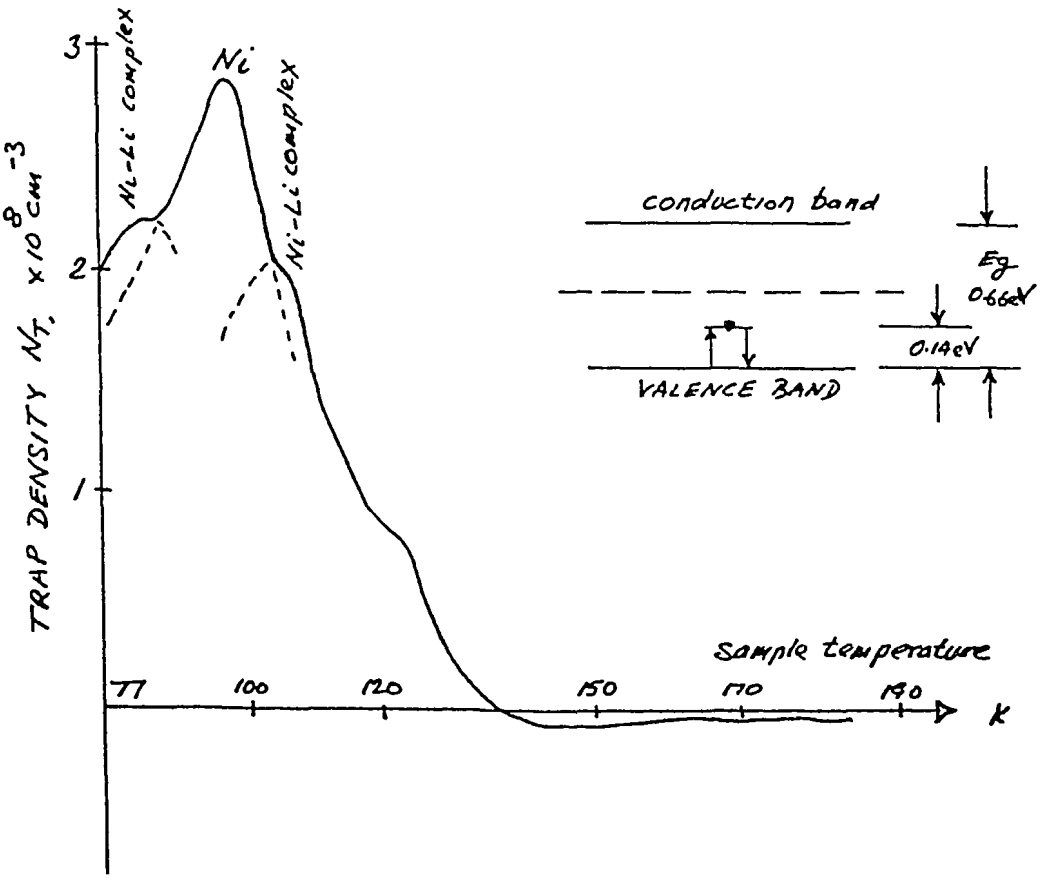

Graph 11 - DLTS scan of HP p-Ge detector diode (full depletion depth)

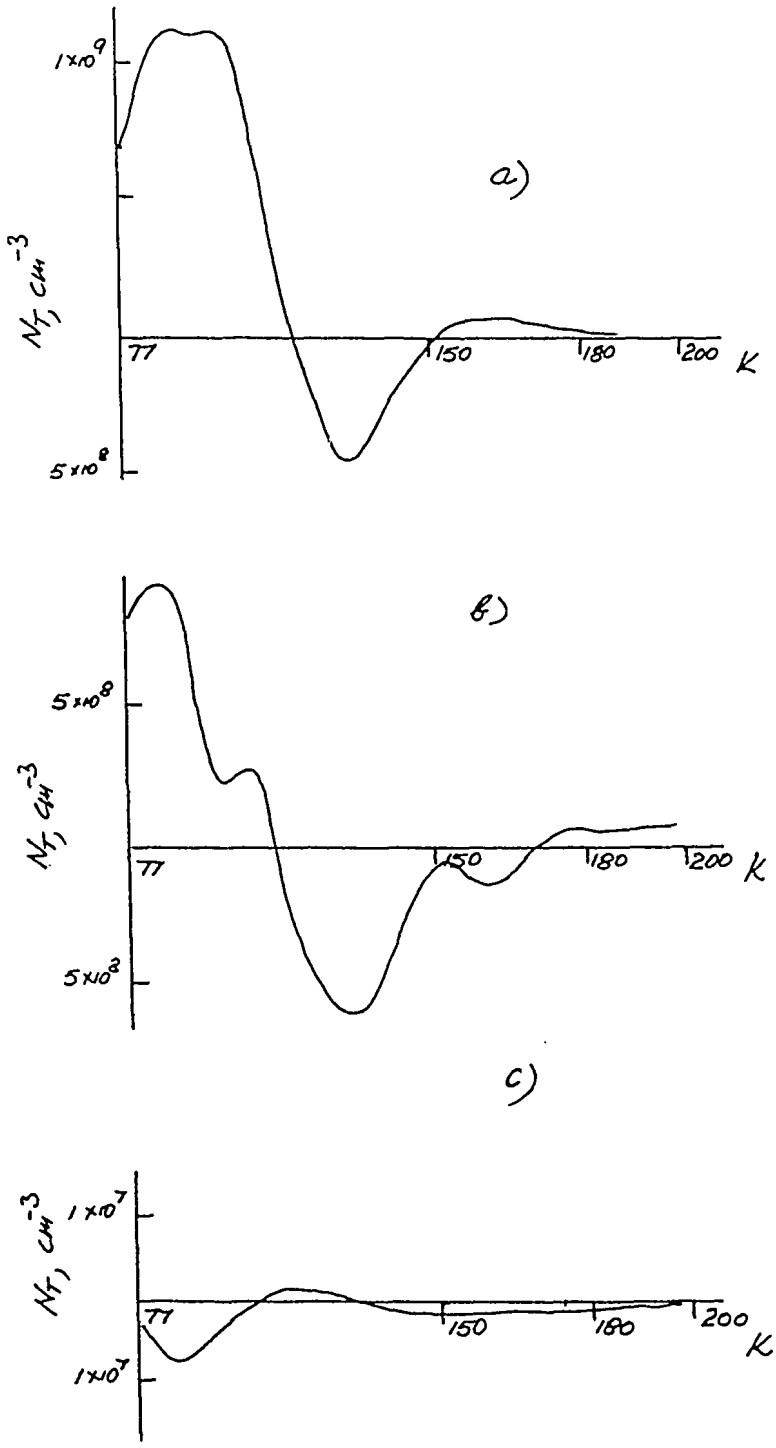

Graph 12 - DLTS spectrum - neutralisation of defect

(a) DLTS after a-Ge:H film deposited on Ge diode

(b) H_2 only, 1.5 hr/150°C

(c) H^+ (plasma), 1.5 hr/150°C shows bulk donor at 10^7 cm^{-3}

Typical result for a-Si:H deposition

Initial surface preparation

Same as for a-Ge:H.

Film deposited

Same as for a-Ge:H.

$I_R(V_R)$ at 77 K

All cases showed remarkable diode characteristics. Diode would be suitable as a detector.

DLTS spectrum

Showed no generated surface defects, graph 13 shows only bulk $/N_A - N_D/$ concentration. The DLTS spectrum showed no contributed acceptor level as found in the a-Ge:H film deposition.

7. CONCLUSION

The experimental work for this project involved some four months. During that time, a number of different innovations were tried with varying success.

Successful Ge γ-ray detector diodes were built and common isotopes resolved. Spectral resolution lines were measured and showed marked superiority compared to that from conventionally prepared detectors.

Hydrogenation of surface states proved to be very successful, as other workers have found. Such processes will undoubtedly be used in future Ge detector fabrication.

Surface passivation studies revealed unexpected hole trapping defects generated when a-Ge:H film is applied. No defect traps were found when using a-Si:H films and preliminary results suggest that such films will be good passivants. The a-Si:H films were found to be mechanically strong, but regretfully, tests into their imperviousness to gaseous cryogenic desorption impurities (such as H_2O vapour) were not carried out due to the termination of the project.

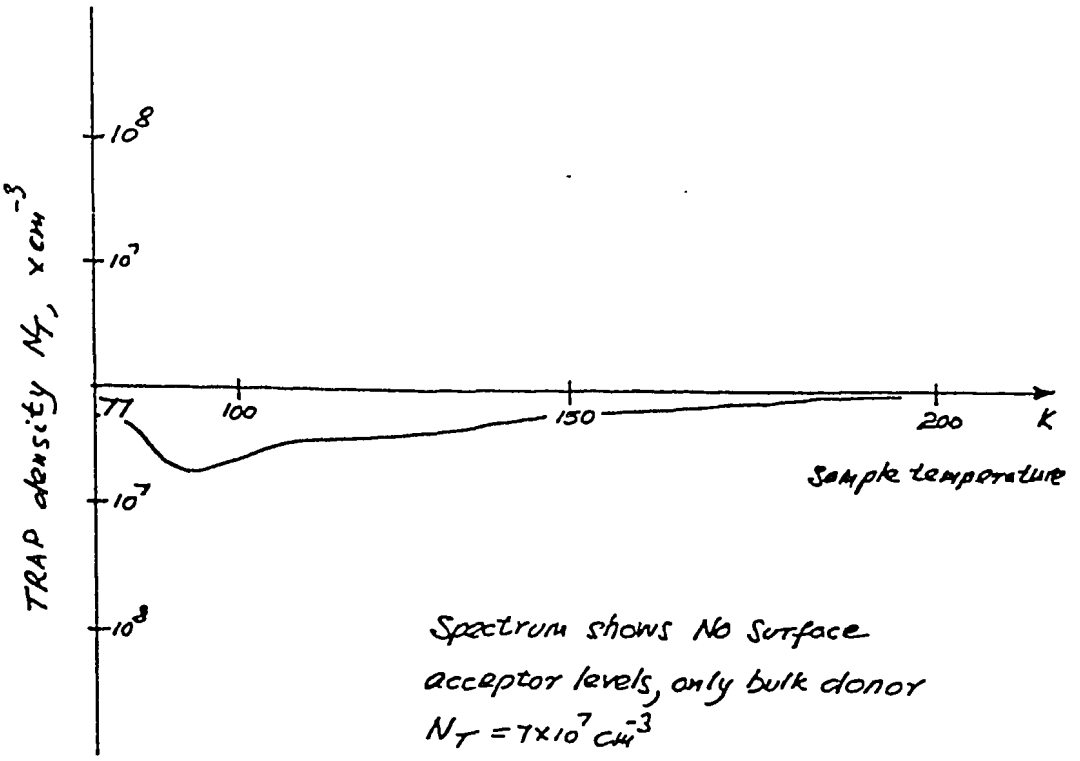

Graph 13 - DLTS spectrum of a-Si:H deposited on HP Ge diode

Systems developed during the project have been reliable and will be used in future work, possibly on solar cell experimentation and further passivation experiments. Passivation of the p-n junction itself has been considered and will be attempted as a follow through project at Ansto in the next few months.

8. ACKNOWLEDGEMENTS

We would like to acknowledge the continuing support of Dr J Boldeman into this work.

9. REFERENCES

[1] Haller, E.E. and Hansen, W.L. (1973) - Lawrence Berkeley Laboratory Report, LBL-1744.

[2] Vogel, F.L. Jr. (1955) - Acta Metallurgica 3, 245.

[3] Hubbard, G.S. and Haller, E.E. (1979) - Lawrence Berkeley Laboratory Report, LBL-9342.

[4] Miller, ED 19, No. 10 (1972) - IEEE.

[5] Ewing, J. and Llacer, J. (1974) - IEEE Trans. Nucl. Sci. NS-21, 370.

[6] Hansen, W.L., Haller, E.E. and Hubbard, G.S. (1980) - Vol. NS27, No.1, IEEE.

[7] Wilson, J.I.B., McGill, J. and Wearne, D. (1978) - Advances in Physics, Vol. 77, No.3, pp 385-395.

[8] Hansen, W.J. and Haller, E.E. (1980) - Lawrence Berkeley Laboratory Report, LBL-10726.

[9] Chu Wei-Kan, M. W., and Nicolet, M.A. (1978) - "Backscattering Spectrometry", New York, Academic Press.

[10] Williams, A.W., Pearton, S.J. and Alexiev, D. (1980) - AAEC.TN147.

[11] Pearton, S.J., Alexiev, D., Tavendale, A.J. and Williams, A.A. (1981) - AAEC/E503.

[12] Lang, D.V. (1974) - J. Appl. Phys., 45, 3023.

[13] Miller, G.L., Ramirez, J.V. and Robinson, D.A.H. (1975) - J. Appl. Phys. 46(6) 2638.

[14] Miller, G.L., Lang, D.V. and Kimberling, L.C. (1977) - Ann. Rev. Mat. Sci., pp 377-448.